

Crystal engineering of pharmaceutical co-crystals: “NMR-crystallography” of Niclosamide co-crystals

David Luedeker,[†] Rebecca Gossmann,[‡] Klaus Langer,[‡] and
Gunther Brunklaus^{*,†}

SUPPORTING INFORMATION

[†]Institut für Physikalische Chemie, Westfälische Wilhelms-Universität Münster, Corrensstr. 28, D-48149 Münster, Germany

Fax: (+49)-251-83-36032; email: gbrunklaus@uni-muenster.de

[‡]Institut für Pharmazeutische Technologie und Biopharmazie, Westfälische Wilhelms-Universität Münster, Corrensstr. 48, D-48149 Münster, Germany

Table of contents

Figure S1: ¹⁵ N { ¹ H} CP-MAS NMR spectra of NCL and its co-phases	S2
Table S1: Experimental ¹⁵ N chemical shifts of NCL and its co-phases	S2
Figure S2: ¹³ C { ¹ H} CP-MAS NMR spectra of NCL and its co-phases	S3
Figure S3: PXRD pattern of NCL, NCL-BA, NCL-IN, NCL-NA and NCL-IA	S4
Figure S4: PXRD pattern of NCL, NCL-H _A and NCL-H _B	S4
Figure S5: PXRD pattern of NCL, AT, NCL-AT, NCL-AA-I and NCL-AA-II	S5
Figure S6: PXRD pattern of NCL, IN, NCL-BA and NCL-IN	S5
Figure S7: PXRD pattern of NCL, IA, NA, NCL-IA and NCL-NA	S6
Figure S8: Rietveld fit and refinement of NCL-H _A	S6
Figure S9: Crystal packing of NCL-H _A	S7
Figure S10: DSC data of NCL, its co-crystals and reference compounds	S7
Figure S11: Standard curve for the quantification of NCL in solution via HPLC	S8
Figure S12: ¹ H- ¹ H DQ-MAS-NMR spectrum of the NCL-AT co-crystal	S8
Figure S13: ¹ H- ¹ H DQ-MAS-NMR spectrum of the NCL-IA co-crystal	S9
Figure S14: ¹ H- ¹ H DQ-MAS-NMR spectrum of the NCL-NA co-crystal	S9
Figure S15: ¹ H- ¹ H DQ-MAS-NMR spectrum of the NCL-IN co-crystal	S10
Figure S16: ¹ H- ¹ H DQ-MAS-NMR spectrum of the NCL-BA co-crystal	S10
Figure S17: ¹ H- ¹ H DQ-MAS-NMR spectrum of the NCL-AA-II co-crystal	S11
Figure S18: ¹ H- ¹ H DQ-MAS-NMR spectrum of the NCL-AA-I co-crystal	S11

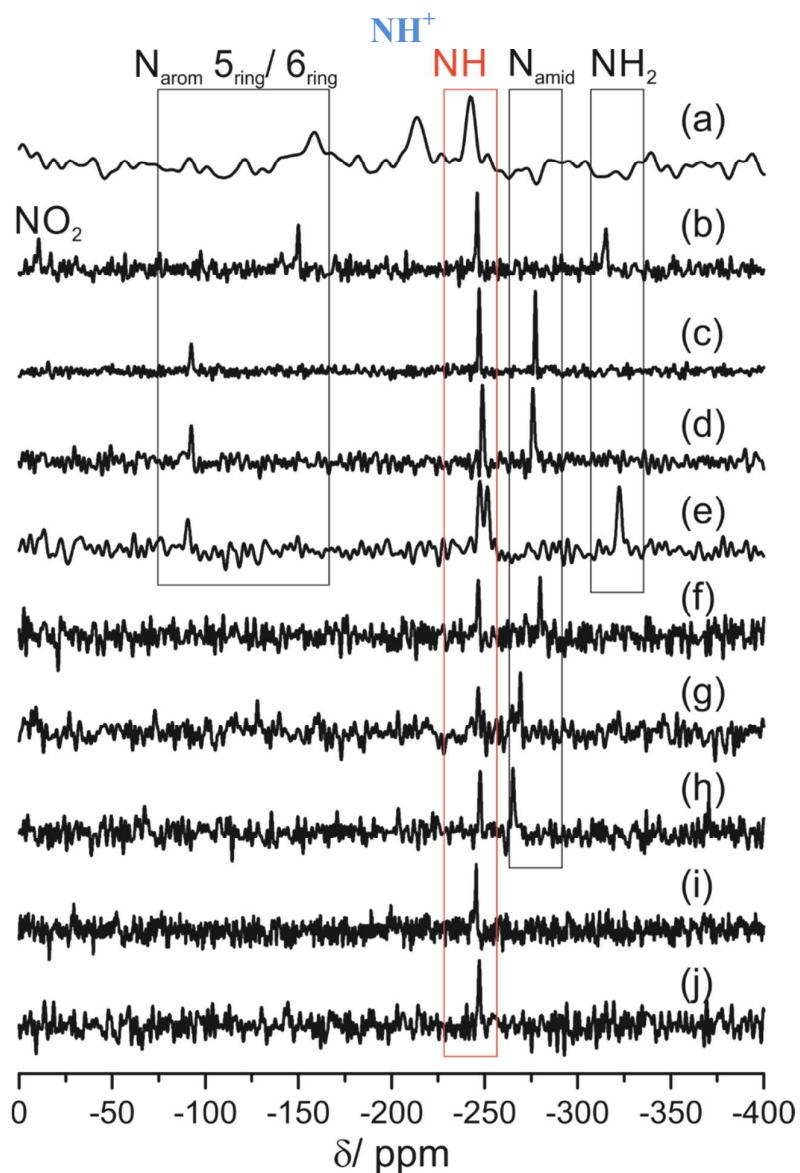


Figure S1: $^{15}\text{N}\{^1\text{H}\}$ -CPMAS-NMR spectra (acquired at 35.5 MHz and 10 kHz spinning frequency) of (a) NCL-IMI, (b) NCL-AT, (c) NCL-IA, (d) NCL-NA, (e) NCL-IN, (f) NCL-BA, (g) NCL-AA-II, (h) NCL-AA-I, (i) NCL- H_A and (j) NCL anhydrate.

Table ST1: Experimental ^{15}N chemical shifts of NCL hydrate H_A and co-crystals.

Phase	$\delta_{\text{iso}}^{15}\text{N}(\text{NH})$ /ppm	$\delta_{\text{iso}}^{15}\text{N}(\text{N}_{\text{amide}})$ /ppm	$\delta_{\text{iso}}^{15}\text{N}(\text{N}_{\text{arom}})$ /ppm	$\delta_{\text{iso}}^{15}\text{N}(\text{NH}_2)$ /ppm
NCL	-247.1	-	-	-
NCL- H_A	-245.5	-	-	-
NCL-AA-I	-247.6	-265.3	-	-
NCL-AA-II	-246.6	-269.2	-	-
NCL-BA	-246.6	-279.9	-	-
NCL-IN	-247.5	-	-90.5	-322.4
NCL-NA	-248.9	-276.1	-92.4	-
NCL-IA	-247.1	-277.3	-92.4	-
NCL-AT	-246.0	-	-149.9	-315.0
NCL-IMI	-242.6		-213.7 NH^+	-158.1 NH

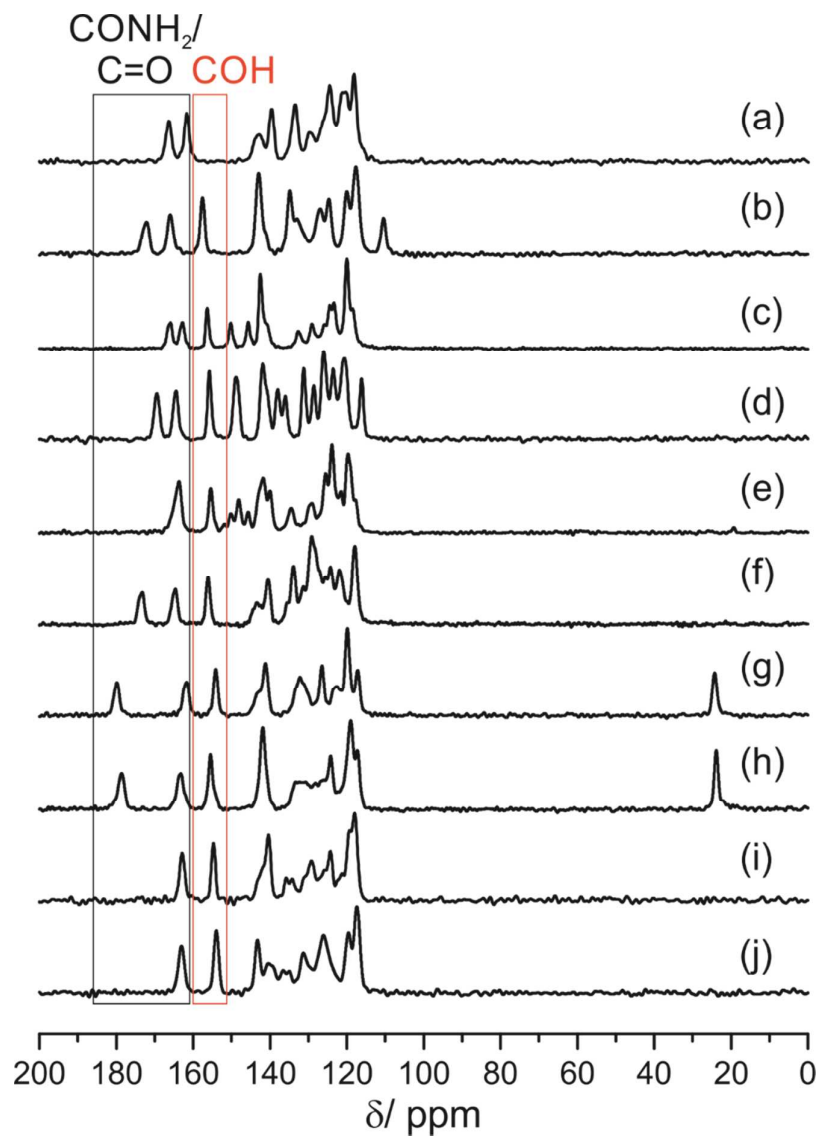


Figure S2: $^{13}\text{C}\{^1\text{H}\}$ -CPMAS-NMR spectra (acquired at 75.5 MHz and 12 kHz spinning frequency) of (a) NCL-IMI, (b) NCL-AT, (c) NCL-IA, (d) NCL-NA, (e) NCL-IN, (f) NCL-BA, (g) NCL-AA-II, (h) NCL-AA-I, (i) NCL- H_A and (j) NCL anhydrate.

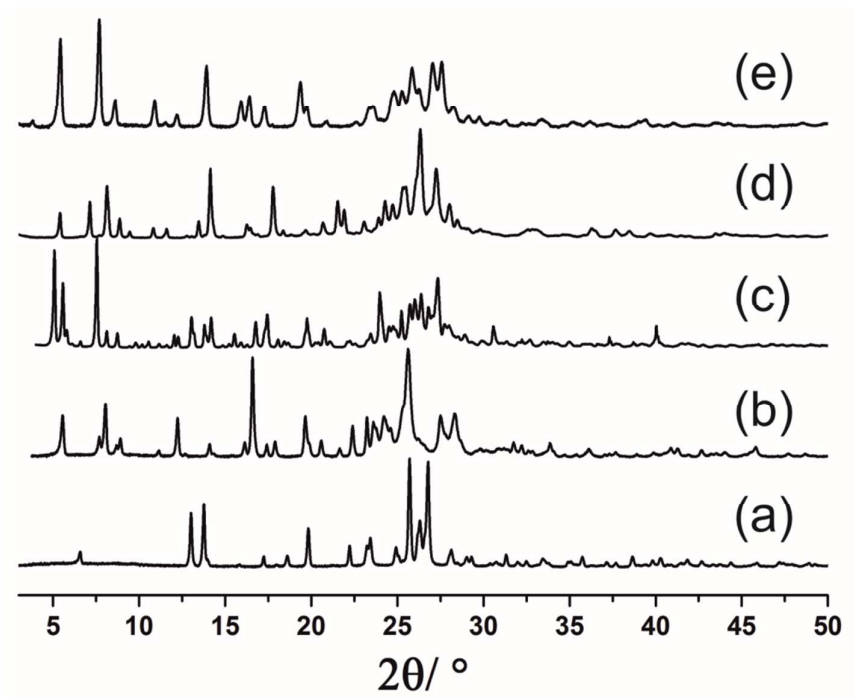


Figure S3: Powder XRD pattern of (a) niclosamide anhydrate (NCL) in comparison to the novel co-crystals of NCL with (b) benzamide (BA), (c) isoniazide (IN), respectively, and the reproduced co-crystals of NCL with (d) nicotinamide (NA) and (e) isonicotinamide (IA).

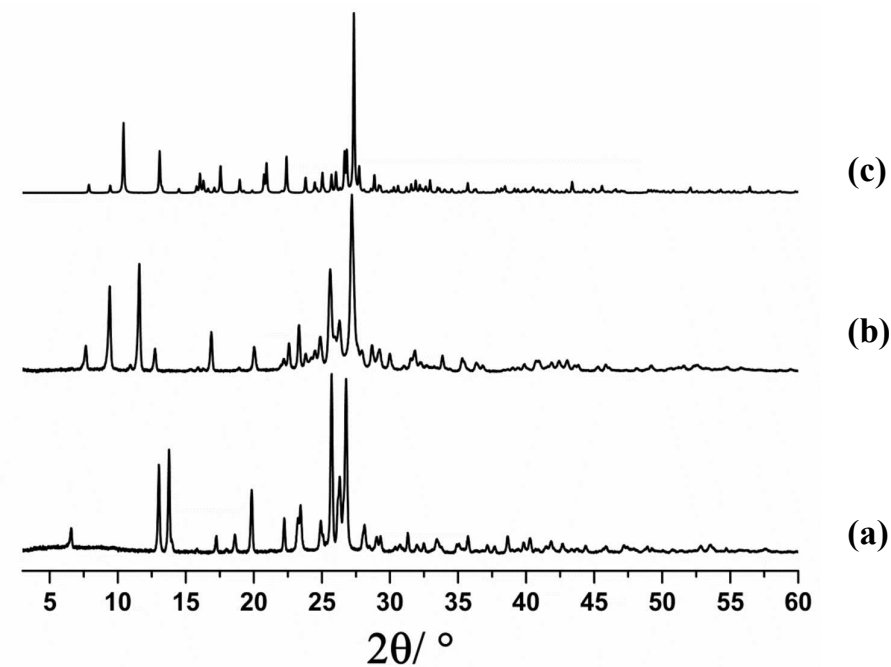


Figure S4: PXRD data of (a) niclosamide anhydrate (NCL), (b) niclosamide hydrate (NCL- H_A), and (c) the theoretical pattern of niclosamide hydrate (NCL- H_B).

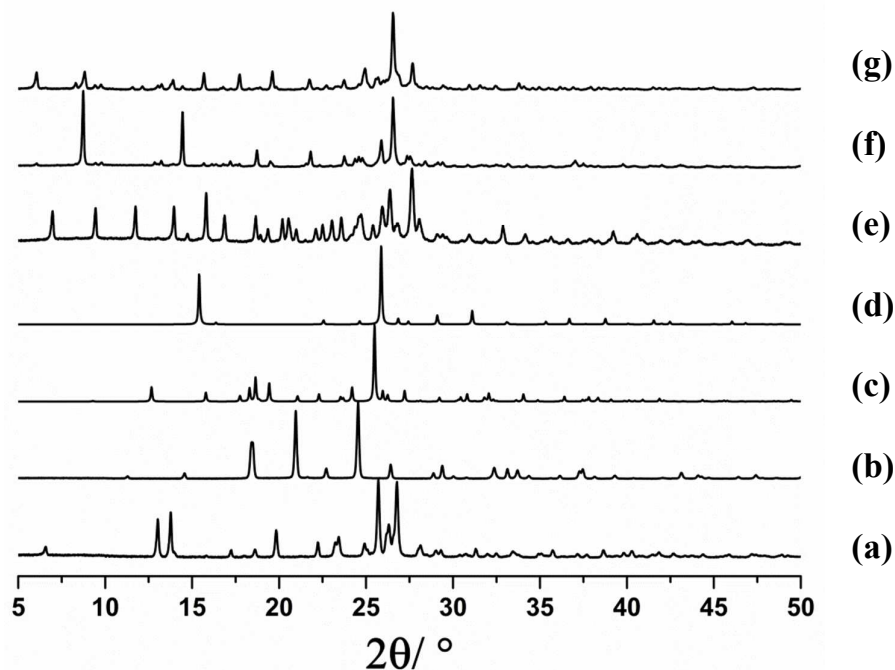


Figure S5: PXR D data of (a) niclosamide anhydrate (NCL), (b) 2-aminothiazole (AT), (c) theoretical pattern of acetamide Pccn (AA), (d) theoretical pattern of acetamide R3c (AA), (e) niclosamide – 2-aminothiazole co-crystal (1:1; NCL-AT), (f) niclosamide – acetamide co-crystal from ethanol (1:1; NCL-AA-I), and (g) niclosamide – acetamide co-crystal from acetone (1:1; NCL-AA-II).

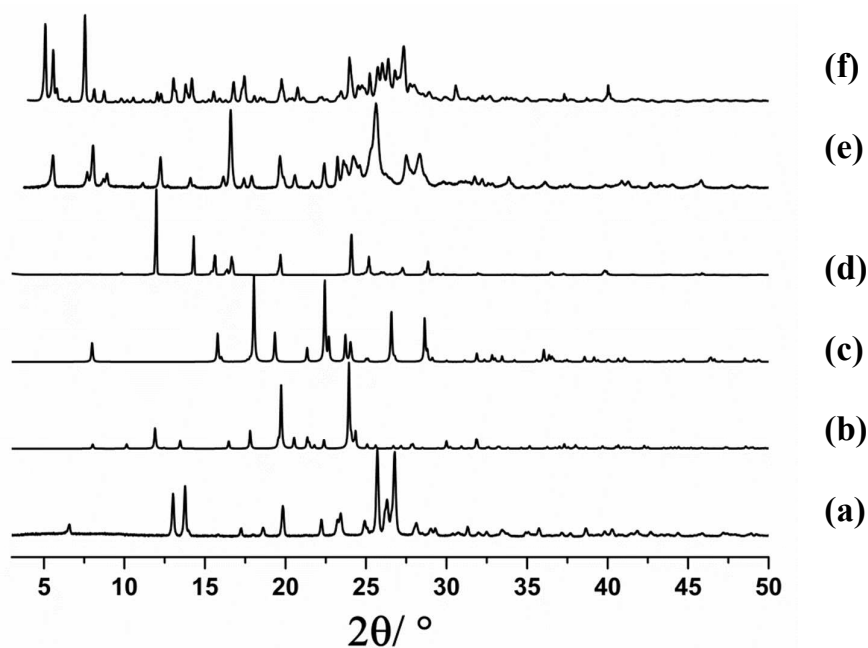


Figure S6: PXR D data of (a) niclosamide anhydrate (NCL), (b) theoretical pattern of benzamide Pba2 (BA), (c) theoretical pattern of benzamide P2₁/c (BA), (d) isoniazide (IN), (e) niclosamide – benzamide co-crystal (1:1; NCL-BA), and (f) niclosamide – isoniazide co-crystal (1:1; NCL-IN).

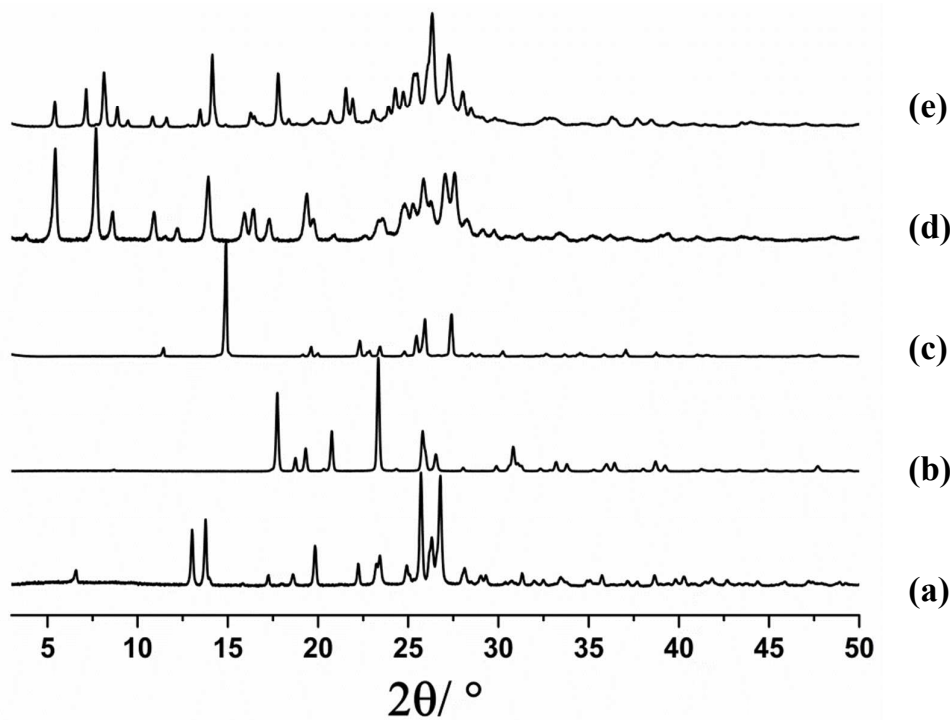


Figure S7: PXRD data of (a) niclosamide anhydrate (NCL), (b) isonicotinamide (IA), (c) nicotinamide (NA), (d) niclosamide – isonicotinamide co-crystal (1:1; NCL-IA), and (e) niclosamide – nicotinamide co-crystal (1:1; NCL-NA).

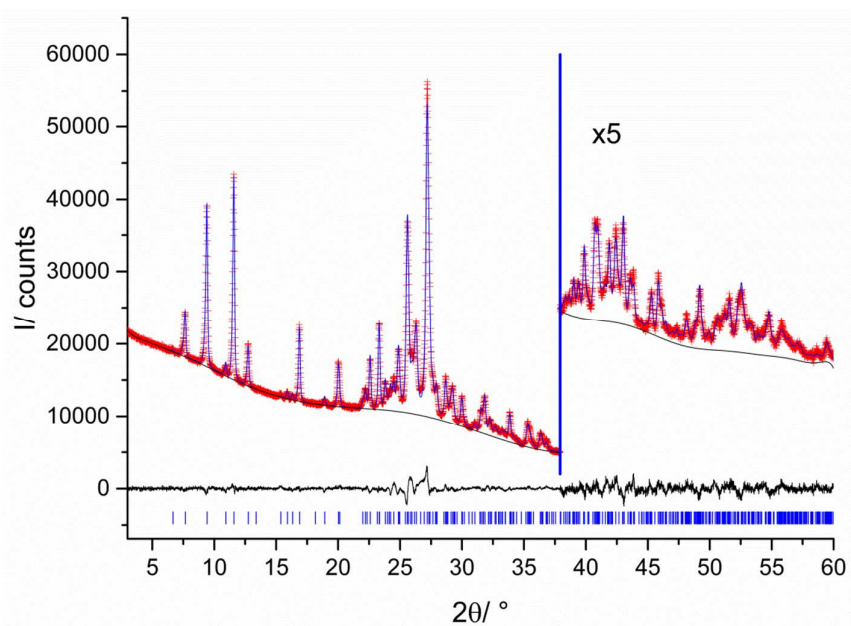


Figure S8: The final Rietveld fit obtained for NCL- H_4 : experimental data points (red), Rietveld refinement fit (blue), background (black line), difference $I_{obs} - I_{calc}$ (black) and phase tick marks (blue). The vertical blue line marks the place at which the data points are multiplied with factor five for better visibility of the data in the higher 2θ region.

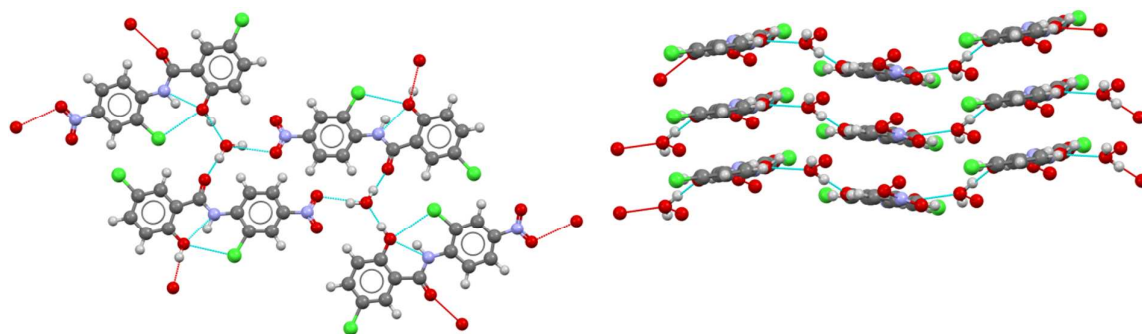


Figure S9: (left) $NCL-H_4$ hydrate forms trimeric layers involving the water molecule containing $C_2^2(8)$ and $C_2^2(14)$ chains. (right) π - π interactions (3.8120 Å) lead to AAA packing of layers along the c -axis.

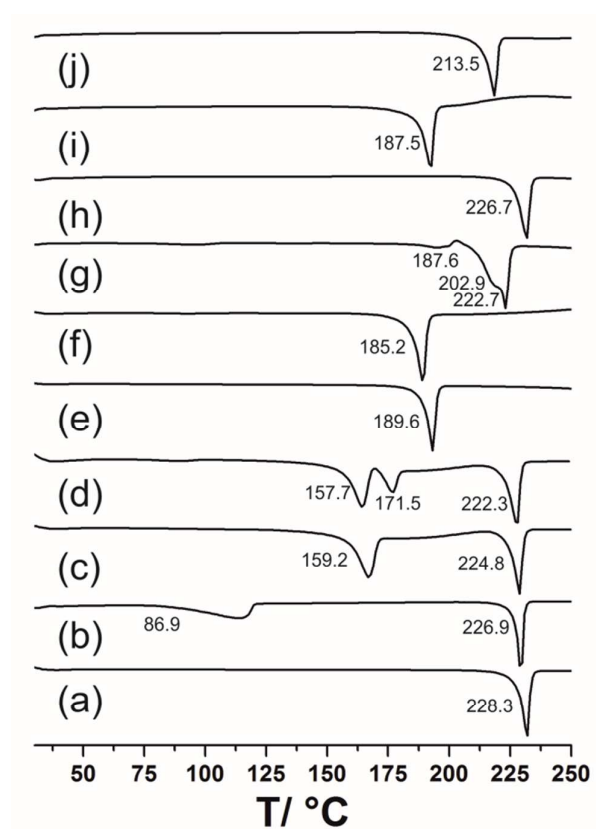


Figure S10: DSC data of (a) niclosamide anhydrate (NCL), (b) niclosamide hydrate ($NCL-H_4$), (c) niclosamide – acetamide co-crystal from EtOH ($NCL-AA-I$), (d) niclosamide – acetamide co-crystal from acetone ($NCL-AA-II$), (e) niclosamide – benzamide co-crystal ($NCL-BA$), (f) niclosamide – isoniazide co-crystal ($NCL-IN$), (g) niclosamide – nicotinamide co-crystal ($NCL-NA$), (h) niclosamide – isonicotinamide co-crystal ($NCL-IA$), (i) niclosamide – 2-aminothiazole co-crystal ($NCL-AT$), and (j) niclosamide – imidazole ($NCL-IMI$).

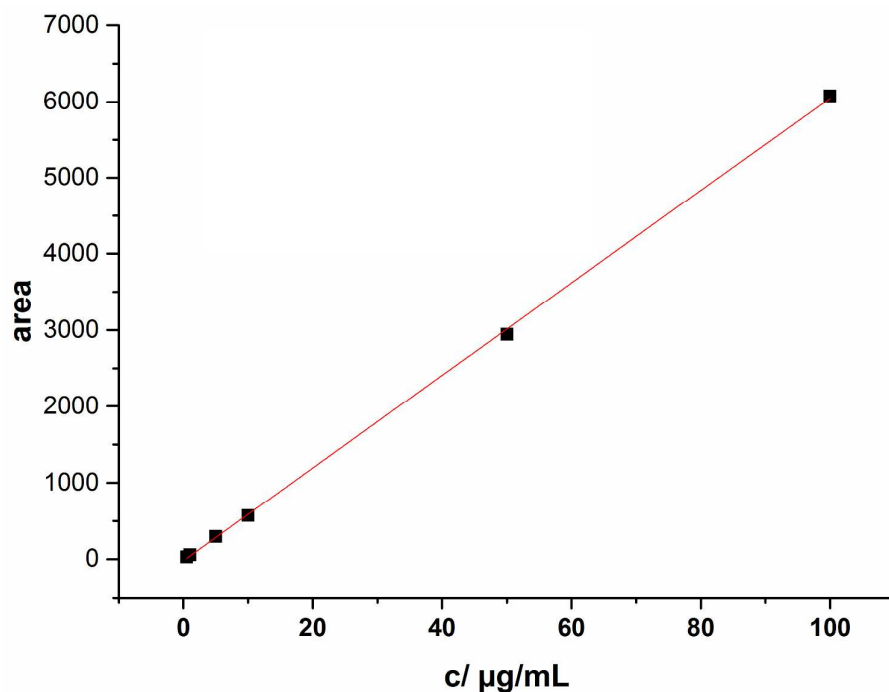


Figure S11: Standard curve for the quantification of NCL in solution via HPLC. The red line reflects the linear fit according to $y = a + b x$, yielding $a = -19.4552$ and $b = 60.4258$ ($R = 0.9998$).

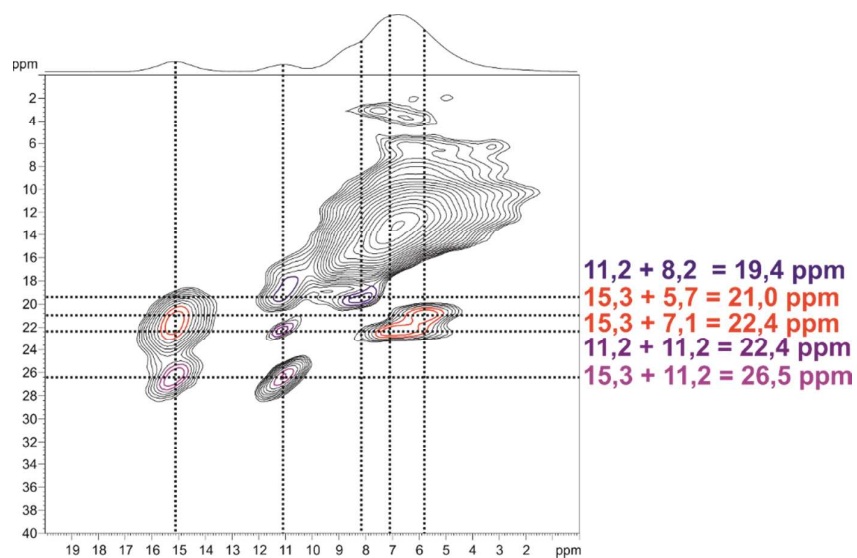


Figure S12: ^1H - ^1H DQ-MAS-NMR spectrum of the NCL-AT co-crystal at 500.1 MHz and 30 kHz MAS. 24 positive contour levels between 1.5% and 100% of the maximum peak intensity were plotted. The F2 projection is shown on top; the most important DQ cross-peaks are highlighted.

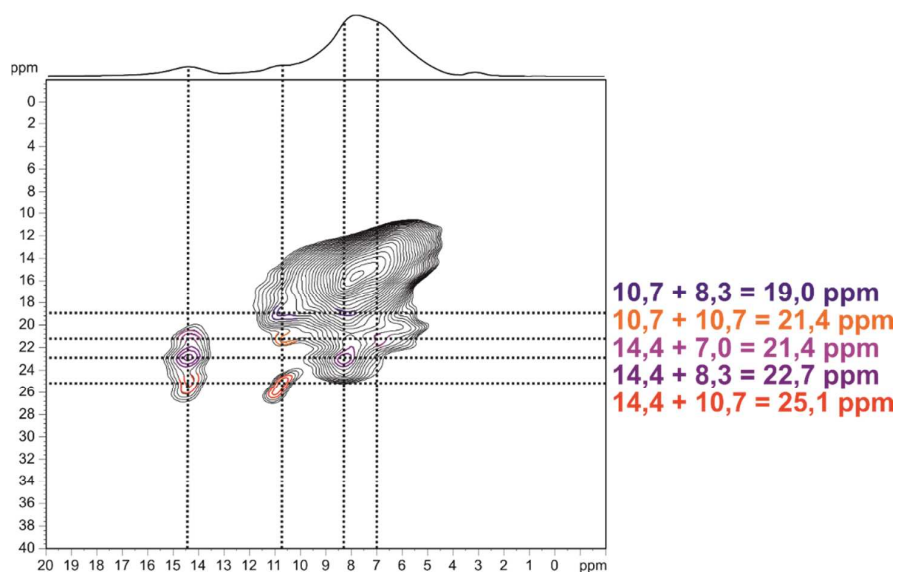


Figure S13: ^1H - ^1H DQ-MAS-NMR spectrum of the NCL-IA co-crystal at 500.1 MHz and 30 kHz MAS. 24 positive contour levels between 1.5% and 100% of the maximum peak intensity were plotted. The F2 projection is shown on top; the most important DQ cross-peaks are highlighted.

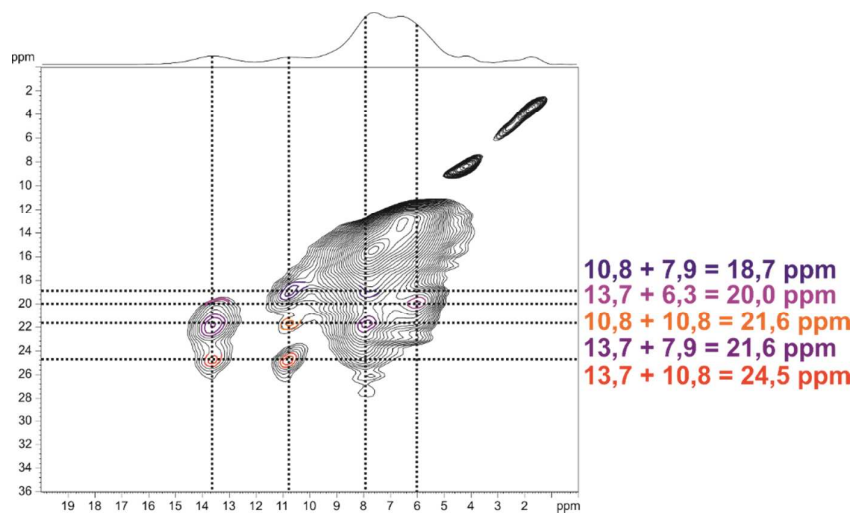


Figure S14: ^1H - ^1H DQ-MAS-NMR spectrum of the NCL-NA co-crystal at 500.1 MHz and 30 kHz MAS. 24 positive contour levels between 1.5% and 100% of the maximum peak intensity were plotted. The F2 projection is shown on top; the most important DQ cross-peaks are highlighted.

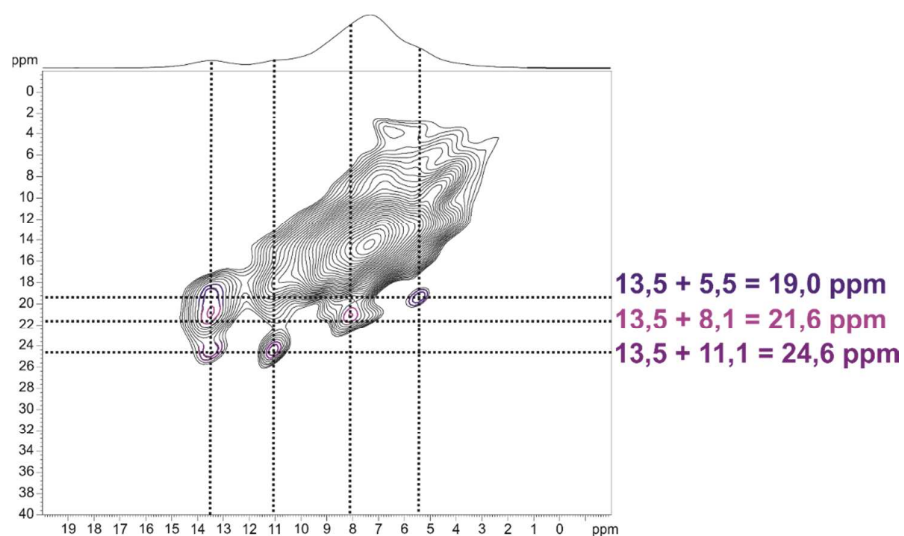


Figure S15: ^1H - ^1H DQ-MAS-NMR spectrum of the NCL-IN co-crystal at 500.1 MHz and 30 kHz MAS. 24 positive contour levels between 1.5% and 100% of the maximum peak intensity were plotted. The F2 projection is shown on top; the most important DQ cross-peaks are highlighted.

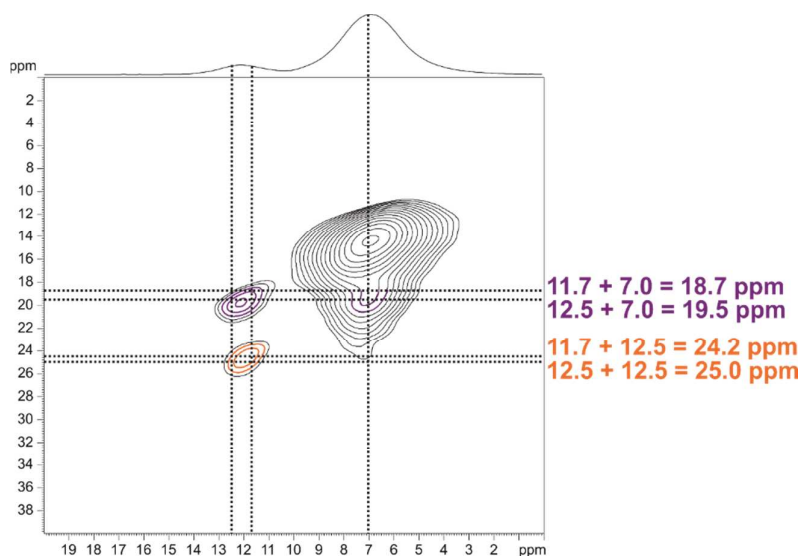


Figure S16: ^1H - ^1H DQ-MAS-NMR spectrum of the NCL-BA co-crystal at 500.1 MHz and 30 kHz MAS. 24 positive contour levels between 1.5% and 100% of the maximum peak intensity were plotted. The F2 projection is shown on top; the most important DQ cross-peaks are highlighted.

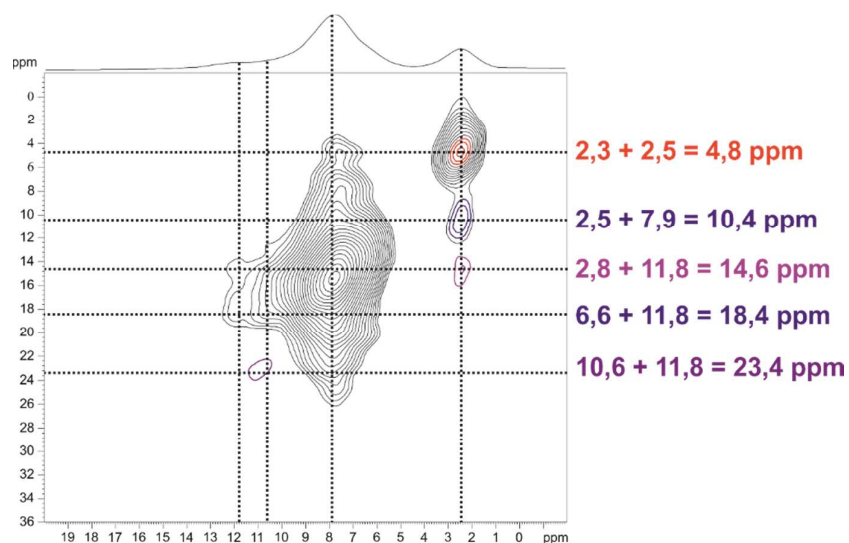


Figure S17: ^1H - ^1H DQ-MAS-NMR spectrum of the NCL-AA-II co-crystal at 500.1 MHz and 30 kHz MAS. 24 positive contour levels between 1.5% and 100% of the maximum peak intensity were plotted. The F2 projection is shown on top; the most important DQ cross-peaks are highlighted.

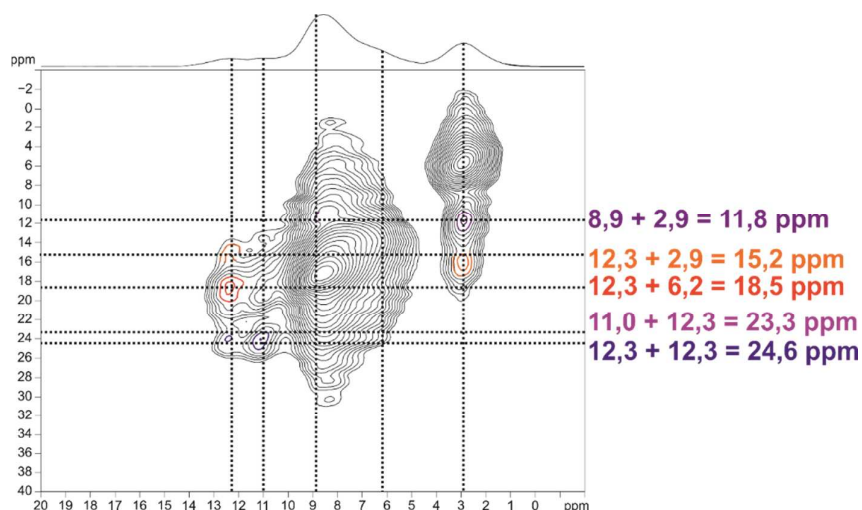


Figure S18: ^1H - ^1H DQ-MAS-NMR spectrum of the NCL-AA-I co-crystal at 500.1 MHz and 30 kHz MAS. 24 positive contour levels between 1.5% and 100% of the maximum peak intensity were plotted. The F2 projection is shown on top; the most important DQ cross-peaks are highlighted.